Image and Video Dehazing using View-based Cluster Segmentation

Feng Yu, Chunmei Qing*, Xiangmin Xu, Bolun Cai
School of Electronic and Information Engineering, South China University of Technology, Guangzhou, China

***Abstract*—To avoid distortion in sky regions and make the sky and white objects clear, in this paper we propose a new image and video dehazing method utilizing the view-based cluster segmentation. Firstly, GMM(Gaussian Mixture Model)is utilized to cluster the depth map based on the distant view to estimate the sky region and then the transmission estimation is modified to reduce distortion. Secondly, we present to use GMM based on Color Attenuation Prior to divide a single hazy image into K classifications, so that the atmospheric light estimation is refined to improve global contrast. Finally, online GMM cluster is applied to video dehazing. Extensive experimental results demonstrate that the proposed algorithm can have superior haze removing and color balancing capabilities.**

***Index Terms*—image dehazing, video dehazing, GMM, dark channel prior, view-based cluster segmentation**

I. Introduction

Outdoor images taken in bad weather usually lose contrast and fidelity. Most automatic systems, which strongly depend on the definition of the input images, fail to work normally caused by the degraded images. Therefore, improving the technique of image haze removal will benefit some applications such as object identification or target positioning. Dehazing is the process of removing haze from hazy images and enhancing the image contrast. Early, histogram equalization or unsharp masking is employed to enhance the image contrast by stretching the histogram [1]. However, the dehazing effect is limited. Later, several dehazing algorithms have been proposed to estimate object depths using multiple images or additional information. For example, object depths are estimated from two images with different degrees of polarization [2]. These algorithms can remove haze effectively, but require multiple images or additional information limiting their applications.

Based on a large number of experiments on haze-free images, He et al. [3] discover the dark channel prior, where at least one color channel has some pixels whose intensities are very low and close to zero in most of the non-sky patches. With this prior, they can restore the haze-free image well by the atmospheric scattering model in most cases. But it can't well handle the sky images. Meng et al. [4] propose an effective regularization dehazing method to restore the haze-free image by exploring the inherent boundary constraint. Zhu et al. [5] create a linear model for modeling the scene depth to recover the hazy image well. Tarel et al. [6] apply median of median filter to improve computational efficiency.

However, these current methods still have some shortcomings: 1) the inaccurate transmission estimation for sky regions leads to distortion; 2) only one unified estimation of atmospheric light for the hazy image results in local oversaturation. In order to solve these two issues, an image and video dehazing method is proposed using the view-based cluster segmentation. The main contributions of this paper are highlighted as follows: 1) view-based cluster segmentation is proposed by using GMM cluster and Color Attenuation Prior for the depth map and the hazy image separately; 2) the transmission estimation and the atmospheric light estimation are modified using the view-based cluster segmentation to decrease color distortion and improve global contrast; 3) video dehazing algorithm is presented by using online GMM cluster.

* Chunmei Qing is the corresponding author. Email: qchm@scut.edu.cn.

II. Image Dehazing

A. Haze Modeling

In this paper, we adopt the haze image formation model proposed by Koschmieder [7], which has been widely used in previous works [3], [4], [5], as follows

$$I^c(x) = J^c(x)\,t(x) + A^c\left(1 - t(x)\right), \tag{1}$$

where, $I^c(x)$, $c \in \{r, g, b\}$ is the observed intensity, $J^c(x)$ is the real scene to be recovered, $t(x)$ is the medium transmission, and A^c is the global atmospheric light. Therefore, once the transmission map $t(x)$ and the atmospheric light A^c are determined, the original image $J^c(x)$ could be restored as

$$J(x) = \frac{I^c(x) - A^c}{\max\left(t(x), t_0\right)} + A^c, \tag{2}$$

when the refined transmission $t(x)$ is close to zero, the directly recovered scene radiance $J^c(x)$ is prone to be noise. So we restrict the transmission $t(x)$ to a lower bound. Typically, we choose $t_0 = 0.1$ as suggested in [3].

B. Proposed view-based cluster segmentation

Before we present the proposed method, we briefly introduce the GMM and some notations which we will utilize later. GMM [8] is modeled by a K Gaussian component mixing model with mixing proportions $\{\pi_k\}$. The probability density function is

$$p\left(f(x)\right) = \sum_{k=1}^{K} p(k)p\left(f(x)\,|k\right) = \sum_{k=1}^{K} \pi_k \mathcal{N}\left(f(x)\,|\mu_k, \sigma_k\right), \tag{3}$$

The log-likelihood function of Equ. (3) is given by

$$\lambda = \sum_{x=1}^{N} \log\left\{p\left(f(x)\right)\right\}. \tag{4}$$

978-1-5090-5316-2/16/$31.00 © 2016 IEEE

In order to find the model parameter $\{\mu_k, \sigma_k, \pi_k\}$ to make the Equ. (4) maximize, the expectation-maximization (EM) algorithm is utilized. In EM, we calculate the posteriori probability $\gamma(f(x), k)$ as follow

$$\gamma(f(x), k) = \frac{\pi_k \mathcal{N}(f(x) | \mu_k, \sigma_k)}{\sum_{i=1}^{K} \pi_k \mathcal{N}(f(x) | \mu_i, \sigma_i)}, \tag{5}$$

where the model parameter $\{\mu_k, \sigma_k, \pi_k\}$ is calculated by

$$\begin{cases} \pi_k = N_k/N = \sum_{x=1}^{N} \gamma(f(x), k) \Big/ N \\ \mu_k = \frac{1}{N_k} \sum_{x=1}^{N} \gamma(f(x), k) f(x) \\ \sigma_k = \frac{1}{N_k} \sum_{x=1}^{N} \gamma(f(x), k) (f(x) - \mu_k) (f(x) - \mu_k)^T \end{cases} \tag{6}$$

Here N is the number of observations, $N_k = \sum_{x=1}^{N} \gamma(f(x), k)$.

We go through a limited number of Equ. (4)(6)(5)$'s$ iterations till the log-likelihood function is convergence.

1) View-based cluster segmentation of the depth map: Since the concentration of the haze increases along with the change of the scene depth $d(x)$ in general. Ideally, the range of the scene depth $d(x)$ is $[0, +\infty)$. It means that when the scenery objects that appear in the image are very far from the observer, the pixel belonging to the region with a distant view in the image should have a large depth, such as the sky region. This motivates us to cluster the depth map, which is obtained as in [5], based on the distant view of observer so that the sky region can be segmented out. That means we have $f(x) = d(x)$ and $K = 2$ in the GMM model. Some clustered results are shown in Fig.1(a), where the sky region is well segmented based on the depth map.

2) View-based cluster segmentation of the hazy image: Because the difference of the depth between the adjacent pixels is small in the nonsky region, they don't have clear dividing, so we can't get the good segmentation of the hazy image. However, the color attenuation prior provided by Zhu et al.[5] represents the difference between the brightness $v(x)$ and the saturation $s(x)$ of scene increases along with the haze concentration $h(x)$, and the change of the difference is big along with the various concentration of the haze. This motivates us to cluster the difference between the brightness and the saturation to divide a hazy image into K clusters, which present variously dense view segmentations of a single hazy image. Cluster # k is resorted according to the concentration of the haze, which means k increases progressively by the decrease of the mean value μ_k. We have $f(x) = v(x) - s(x)$ and when one of mean values μ_k for cluster $K+1$ is zero, the number of cluster K can be determined. Some clustered results are shown in Fig. 1(b), where more distance views are segmented based on more clusters.

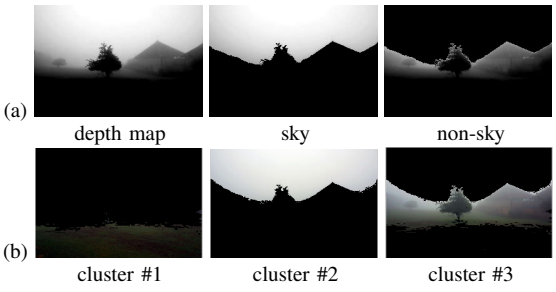

Fig. 1. View-based cluster segmentation results

C. Modified Transmission Map Estimation

The dark channel of J^c is close to zero due to the dark channel prior [3]

$$J^{dark}(x) = \min_{y \in \Omega(x)} \left(\min_{c \in \{r,g,b\}} J^c(y) \right) = 0, \tag{7}$$

where $\Omega(x)$ is a local patch centered at x, and the block size is 15×15.

With the dark channel prior, the coarse transmission $\tilde{t}(x)$ can be easily obtained by the following equation

$$\tilde{t}(x) = 1 - \omega \min_{y \in \Omega(x)} \left(\min_{c} \frac{I^c(y)}{A^c} \right), \tag{8}$$

ω is a constant parameter representing a small amount of haze kept for distant objects. A typical value of the parameter ω is 0.95. However, the blocking artifacts appear in the image because of space minimum filter. To refine the transmission map, the guided image filtering [9] is applied to smooth the image to get the refined transmission $t'(x)$.

However, the recovery of bright regions such as sky is oversaturation by dark channel prior. So in this paper we propose to refine the transmission of the sky region, which is segmented in the Sec. II-B2. After obtaining above transmission, we adjust the transmission of sky region as in [10].

$$t(x) = \min \left(\max \left(\frac{M}{\underset{c}{mean}(|I^c(x) - A^c|)}, 1 \right) t'(x), 1 \right), \tag{9}$$

where M is a parameter, in the sky region, M may be 10 or 80, which is determined by the sky regions intensity, while in the nonsky region, M equals zero.

D. Modified Atmospheric Light Estimation

Atmospheric light is caused by the scattering of environmental, including direct sunlight, diffuse sky light and light reflected, so it is different in the different clusters of image. In this paper, we respectively obtain the atmospheric light of every cluster. We assume that the atmospheric light estimation of these clusters is $A_1^c, ..., A_k^c$ corresponding to cluster # 1, ..., cluster # k obtained in subsection 2.2.2. The difference among the atmospheric light estimation of these clusters in image is small and the atmospheric light estimation of these clusters is closely correlate, so the atmospheric light can be estimated as

$$\begin{aligned} &A_1^c = \tilde{A}_1^c, \\ &A_k^c = \alpha_k \tilde{A}_k^c + \beta_k A_{k-1}^c + \delta_k, s.t. \alpha_k + \beta_k = 1, \end{aligned} \tag{10}$$

where $\alpha_k, \beta_k, \delta_k$ denotes the adjustment factor of the degree of influence. $\alpha_k, \beta_k, \delta_k$ can be obtained by the least squares method as following

$$(\alpha_k^*, \beta_k^*, \delta_k^*) = \underset{\alpha_k, \beta_k, \delta_k}{\arg\min} \sum\nolimits_{c \in \{r,g,b\}} \left(A_k^c - \tilde{A}_k^c \right)^2, \tag{11}$$

TABLE I
RESULTS OF THE SSEQ ON THE ABOVE IMAGES IN FIG. 2

Methods	Hazy	[6]	[4]	[12]	[5]	[3]	Ours
Canyon	9.76	5.43	**3.41**	9.30	5.53	5.68	5.05
House	3.68	5.91	7.05	**2.12**	6.21	3.18	2.22
Ny2	16.15	17.71	19.68	17.94	15.82	16.11	**15.67**
Ny3	10.16	13.35	14.43	10.39	8.48	9.20	**7.86**
Average	9.93	10.60	11.14	9.93	9.01	8.54	**7.70**

for $\tilde{A}_k^c$, we use the dark channel method [3] to detect the most haze-opaque region of cluster #k and then improve the background light estimation. The top 0.1 percent brightest pixels are picked in the dark channel of cluster #k. Among these pixels, the pixels with highest intensity in the cluster #k are selected as the background light $\tilde{A}_k^c$.

III. VIDEO DEHAZING

For the video dehazing, if we use the above static image method to dehaze video, we will take a lot of time to process the GMM. We propose an alternative way to solve the problem. Obviously, the main time comes from the reasonable choice of initial parameters for GMM and the number of clusters. Because the video is captured in the same environment, the features of hazy video sequence is almost same, so we can use online-updated GMM algorithm [11] to update the parameters in the video sequences. Another, we can assume all the video sequences have the same number of clusters as in the first frame. In the video dehazing, the methods of transmission estimation and background light estimation of hazy video sequence are separately the same as the proposed static image dehazing methods in the above sections.

IV. EXPERIMENTAL RESULTS AND EVALUATION

A. Static Image Dehazing

To demonstrate the effectiveness and robustness of our proposed algorithm, we have tested our method on a large number of hazy images. Furthermore, qualitative and quantitative comparisons are given with the state-of-art algorithms including Tarel et al. [6], Meng et al. [4], Sulami et al. [12], Zhu et al. [5] and He et al.[3] in Fig.2 and in Table I.

For qualitative comparisons, actually the sky region dehazed from a hazy image is very challenge. Such as, Fig. 2(b)-(d) and Fig. 2(f) show that most of haze is removed in the restored images and the details of images are kept, but they can't process the sky region well and the restored sky region is much darker or oversaturation. Because the transmission estimation (Tarel et al. [6], Meng et al. [4], Sulami et al. [12] and He et al. [3]) of sky region based on the dark channel prior is invalid when the scene brightness is nearly to the atmospheric light. Another, Fig. 2(b) and Fig. 2(d) show the recovery of the nonsky region is also poor or is oversaturated, because the airlight is not well estimated or is sometimes inaccurate. Fig. 2(e) shows Zhu et al. [5] have much denser haze in recovery images. They avoid applying the dark channel prior by direct estimation of depth map, and they assume the scattering coefficient β is 1.0. However, β is not accurate value in a real scenario and it underestimates the haze. Our proposed method can find the sky region and adjust the transmission of it to reduce the distortion. Also, we improve the global contrast reasonably by estimating the atmospheric light of every cluster to reduce the local oversaturation. Therefore, our results are free from oversaturation, and the sky and the cloud are much more clear. We can remove the dense haze in the distance and keep the details of images well.

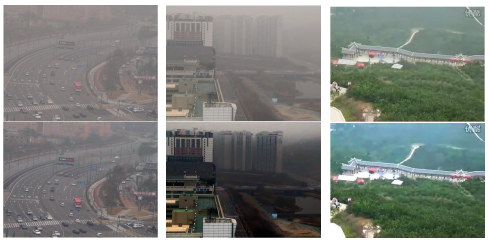

(a) *Cross* (b) *Riverside* (c) *Field*

Fig. 3. The first row is the hazy sequences, and the second is the restored image by our algorithm.

TABLE II
RESULTS OF THE SSEQ ON THE ABOVE VIDEOS IN FIG. 3

Methods	Hazy	[14]	[15]	[3]	ours
Cross	31.56	34.36	34.67	25.73	**25.68**
Riverside	38.91	41.78	41.52	**36.79**	36.94
Field	37.88	38.47	42.56	36.96	**36.61**

For quantitative comparisons, we compare our results with other methods by an image quality assessment system called SSEQ [13]. SSEQ (Spatial Spectral Entropy-based Quality) is an efficient image quality assessment (IQA) model that utilizes local spatial and spectral entropy features on distorted images. We remark the best results by red color and remark the second better results by blue color in Table I. In total, our method demonstrates the best performance.

B. Video Dehazing

We evaluate the performance of the proposed video dehazing algorithm on the *Cross* video (400 frames), *Riverside* video (400 frames), and *Field* video (200 frames) compared with Gibson et al.'s [14], Kim et al.'s [15] and He et al.'s [3]. Fig. 3 shows our proposed algorithm can keep the details of objects, avoid the over-enhancement and improve the global contrast. Table II also illustrates the results by SSEQ. In all, our method demonstrates best performance.

V. CONCLUSIONS

In this paper, we explored and successfully implemented a novel method of image and video dehazing by view-based cluster segmentation. In order to avoid color distortion in sky regions and make the sky and white objects be clear, the proposed algorithm first use the GMM to cluster the depth map to estimate the sky region and then modify the transmission estimation of sky region. Secondly, we present to use GMM based on Color Attenuation Prior to divide a single hazy image into K classifications. Thirdly unlike most previous researches which assume the atmospheric light is only

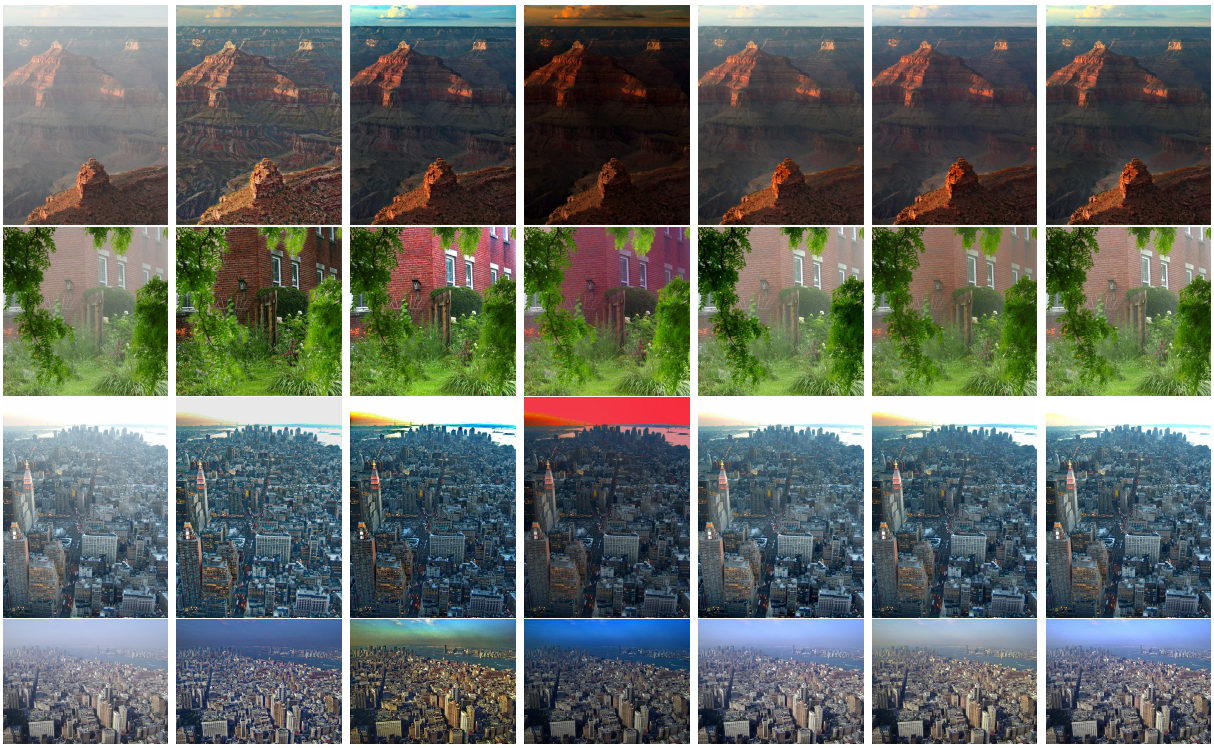

(a) Hazy (b) Tarel's [6] (c) Meng's [4] (d) Sulami's [12] (e) Zhu's [5] (f) He's [3] (g) Ours

Fig. 2. Qualitative comparisons on the hazy images (*Canyon*, *House*, *Ny2*, *Ny3*).

a unified value in the hazy image, we respectively estimate the atmospheric light of each cluster. Therefore, we can increase the global brightness of the dehazed image. Finally, video dehazing method is proposed, which can restore the hazy videos by saving a lot of time for the cluster of sequences of video. A large number of experimental results demonstrate that the proposed algorithm can remove haze effectively and restore the haze images and videos well. It may not invalid when the brightness or the saturation of scene is almost the same in the total image.

ACKNOWLEDGMENT

This work is supported by the National Natural Science Foundation of China (#61401163), Foundation for Distinguished Young Talents in Higher Education of Guangdong (#2014KQNCX015), Guangzhou Key Lab of Body Data Science (#201605030011) and the Fundamental Research Funds for the Central Universities (#2015ZZ032).

REFERENCES

[1] J. A. Stark, "Adaptive image contrast enhancement using generalizations of histogram equalization," *IEEE Transactions on Image Processing*, vol. 9, no. 5, pp. 889–896, 2000.

[2] Y. Y. Schechner, S. G. Narasimhan, and S. K. Nayar, "Instant dehazing of images using polarization," in *IEEE Conference on Computer Vision and Pattern Recognition*, vol. 1, 2001, pp. I–325.

[3] K. He, J. Sun, and X. Tang, "Single image haze removal using dark channel prior," *IEEE Transactions on Pattern Analysis and Machine Intelligence,*, vol. 33, no. 12, pp. 2341–2353, 2011.

[4] G. Meng, Y. Wang, J. Duan, S. Xiang, and C. Pan, "Efficient image dehazing with boundary constraint and contextual regularization," in *IEEE International Conference on Computer Vision*, 2013, pp. 617–624.

[5] Q. Zhu, J. Mai, and L. Shao, "A fast single image haze removal algorithm using color attenuation prior," *IEEE Transactions on Image Processing*, vol. 24, no. 11, pp. 3522–3533, 2015.

[6] J.-P. Tarel and N. Hautiere, "Fast visibility restoration from a single color or gray level image," in *International Conference on Computer Vision*, 2009, pp. 2201–2208.

[7] H. Koschmieder, *Theorie der horizontalen Sichtweite: Kontrast und Sichtweite*. Keim & Nemnich, 1925.

[8] D. A. Reynolds, T. F. Quatieri, and R. B. Dunn, "Speaker verification using adapted gaussian mixture models," *Digital signal processing*, vol. 10, no. 1, pp. 19–41, 2000.

[9] K. He, J. Sun, and X. Tang, "Guided image filtering," *IEEE Transactions on Pattern Analysis and Machine Intelligence*, vol. 35, no. 6, pp. 1397–1409, 2013.

[10] Z. Shi, J. Long, W. Tang, and C. Zhang, "Single image dehazing in inhomogeneous atmosphere," *Optik-International Journal for Light and Electron Optics*, vol. 125, no. 15, pp. 3868–3875, 2014.

[11] J. Yang, X. Yuan, X. Liao, P. Llull, G. Sapiro, D. J. Brady, and L. Carin, "Gaussian mixture model for video compressive sensing," in *IEEE International Conference on Image Processing*, 2013, pp. 19–23.

[12] M. Sulami, I. Glatzer, R. Fattal, and M. Werman, "Automatic recovery of the atmospheric light in hazy images," in *IEEE International Conference on Image Processing*, 2014, pp. 1–11.

[13] L. Liu, B. Liu, H. Huang, and A. C. Bovik, "No-reference image quality assessment based on spatial and spectral entropies," *Signal Processing: Image Communication*, vol. 29, no. 8, pp. 856–863, 2014.

[14] K. B. Gibson, D. T. Vo, and T. Q. Nguyen, "An investigation of dehazing effects on image and video coding," *IEEE Transactions on Image Processing*, vol. 21, no. 2, pp. 662–673, 2012.

[15] J.-H. Kim, W.-D. Jang, J.-Y. Sim, and C.-S. Kim, "Optimized contrast enhancement for real-time image and video dehazing," *Journal of Visual Communication and Image Representation*, vol. 24, no. 3, pp. 410–425, 2013.